ELSEVIER

Physica A 284 (2000) 246–264

PHYSICA A

www.elsevier.com/locate/physa

Anomalous behaviour of hydrodynamic modes in the two dimensional shear flow of a granular material

V. Kumaran*

Department of Chemical Engineering, Indian Institute of Science, Bangalore 560 012, India

Received 12 October 1999; accepted 28 March 2000

Abstract

The growth rates of the hydrodynamic modes in the homogeneous sheared state of a granular material are determined by solving the Boltzmann equation. The steady velocity distribution is considered to be the product of the Maxwell–Boltzmann distribution and a Hermite polynomial expansion in the velocity components; this form is inserted into the Boltzmann equation and solved to obtain the coefficients of the terms in the expansion. The solution is obtained using an expansion in the parameter $\varepsilon = (1 - e)^{1/2}$, and terms correct to ε^4 are retained to obtain an approximate solution; the error due to the neglect of higher terms is estimated at about 5% for $e = 0.7$. A small perturbation is placed on the distribution function in the form of a Hermite polynomial expansion for the velocity variations and a Fourier expansion in the spatial coordinates; this is inserted into the Boltzmann equation and the growth rate of the Fourier modes is determined. It is found that in the hydrodynamic limit, the growth rates of the hydrodynamic modes in the flow direction have unusual characteristics. The growth rate of the momentum diffusion mode is positive, indicating that density variations are unstable in the limit $k \to 0$, and the growth rate increases proportional to $|k|^{2/3}$ in the limit $k \to 0$ (in contrast to the k^2 increase in elastic systems), where k is the wave vector in the flow direction. The real and imaginary parts of the growth rates corresponding to the propagating also increase proportional to $|k|^{2/3}$ (in contrast to the k^2 and k increase in elastic systems). The energy mode is damped due to inelastic collisions between particles. The scaling of the growth rates of the hydrodynamic modes with the wave vector l in the gradient direction is similar to that in elastic systems.

PACS: 05.20; 46.01+z; 62.90+k

Keywords: Granular materials; Shear flow; Hydrodynamic modes; Boltzmann equation

* Fax: +91-80-334-1683.

E-mail address: kumaran@chemeng.iisc.ernet.in (V. Kumaran).

0378-4371/00/$ - see front matter
PII: S0378-4371(00)00199-0

1. Introduction

The homogeneous shear flow of a granular material is a widely studied example of rapid granular flows. In this system, a non-equilibrium steady state is maintained due to a balance of the source of energy provided by the macroscopic shear, and the energy dissipation due to inelastic collisions between particles. Kinetic theory techniques [1–4] have been used to obtain macroscopic equations for the sheared state of the system in a manner similar to the derivation of the Navier–Stokes equation for a hard sphere gas from the Boltzmann equation. These descriptions usually assume a form of the correction to the distribution function in a manner similar to the Sonine polynomial expansion in the Chapman–Enskog theory. This expansion is then inserted into the Boltzmann equation and averaged over velocity space to obtain equations for the macroscopic mass, momentum and energy. The resultant equations are similar to that for a gas at equilibrium, with an additional energy dissipation term due to inelastic collisions. Kinetic theory techniques have also been used to determine the boundary conditions for the shear flow [5].

Simulations [6] have suggested that the homogeneous sheared state of the material is unstable, and an initially random configuration evolves into an inhomogeneous state due to the formation of clusters. The stability of the homogeneous sheared state was analysed by Savage [7] and Babic [8]. Using a continuum description based on the mass, momentum and energy conservation equations, a linear stability analysis was used to determine the growth rate of perturbations. Both these studies indicated that the sheared state is unstable for a wide range of parameter values. Subsequent studies [9,10] used a more sophisticated stability analysis where the wave vector of the disturbances were considered to be a function of time, and the wave vector was considered to be turning with the flow. In these studies, the evolution of a suitably defined norm of the disturbance field was analysed to determine the stability of the system. These studies indicated that though the homogeneous sheared state is linearly unstable, the norm of the disturbance field could still be bounded at long times after transients decay, and the homogeneous state could still be stable at long times. All of these studies used a continuum description of the granular flow.

In the present study, the Boltzmann equation is used to determine the dispersion relation of the hydrodynamic modes about the steady sheared state. Though this description is more fundamental than the continuum description, it already contains the assumption of molecular chaos inherent in the Boltzmann equation. In addition, it is assumed that the particle size is small compared to the mean-free path, so that the only relevant length and time scales are the mean-free path and the strain rate. After the Boltzmann equation is scaled by these characteristic length and time scales, the resultant equation depends only on the coefficient of restitution e of the particle collisions. The velocity distribution of the steady sheared state is determined using an expansion in a basis set consisting of Hermite polynomials [11,12]. In addition, a perturbation expansion about $\varepsilon = (1 - e)^{1/2}$ is used for simplicity, and terms correct to $O(\varepsilon^4)$ are

retained in the solution of the steady state. The results indicate that the errors due to the neglect of higher order terms are small for $e \geqslant 0.7$.

The dispersion relation for the homogeneous sheared state is determined by linearising the Boltzmann equation about the steady solution. A Hermite polynomial expansion in velocity space and a Fourier expansion in the real space are used for the perturbation to the distribution function. The number of solutions for the growth rate for a given wave vector in real space is equal to the number of basis functions used in velocity space. Calculations have been carried out with 15, 21 and 28 basis functions. Though the set of solutions for the growth rate depends on the number of basis functions used, it is verified that the growth rates of the hydrodynamic modes converge to values that are independent of the number of basis functions for $e > 0.9$. Though there is a variation of about 10% in the growth rates in the range $0.7 \leqslant e \leqslant 0.9$, when the number of basis functions is varied from 15 to 28, the scaling laws reported here remain unchanged.

2. Steady velocity distribution

It is convenient to define non-dimensional spatial and velocity variables at the outset. The scaled velocity is defined as $\mathbf{u} = \mathbf{U}/T^{1/2}$, where $\mathbf{U}$ is the dimensional peculiar velocity, and the 'granular temperature' T is the mean square velocity scaled by the particle mass. The scaled spatial coordinates are defined as $\mathbf{x} = \mathbf{X}/(nd)^{-1}$, where $(nd)^{-1}$ is the magnitude of the mean free path of a particle, and n and d are the number density (per unit area) and the particle diameter, respectively. The scaled strain rate then becomes $\gamma = \Gamma/(n\,\mathrm{d}T^{1/2})$, where Γ is the dimensional strain rate. The velocity distribution function, $f(\mathbf{x},\mathbf{u},t)$, is defined such that $f(\mathbf{x},\mathbf{u},t)\,\mathrm{d}\mathbf{x}\,\mathrm{d}\mathbf{u}$ is the number of particles in the differential volume $\mathrm{d}\mathbf{x}$ about $\mathbf{x}$ in real space and $\mathrm{d}\mathbf{u}$ about $\mathbf{u}$ in velocity space. For a steady homogeneous flow, $f(\mathbf{x},\mathbf{u},t) = F(\mathbf{u})$ is only a function of particle velocity. The conservation equation for this distribution function, in the absence of spatial gradients in position and velocity, is

$$-\gamma \frac{\partial u_x F(\mathbf{u})}{\partial u_y} = \frac{\partial_c F(\mathbf{u})}{\partial t}\,, \tag{1}$$

where the collision integral is given by

$$\frac{\partial_c F(\mathbf{u})}{\partial t} = \int_{\mathbf{u}^*} \int_{\mathbf{k}} (e^{-2} F(\mathbf{u}_b) F(\mathbf{u}_b^*) - F(\mathbf{u}) F(\mathbf{u}^*)) \mathbf{w}\cdot\mathbf{k} \tag{2}$$

where $\int_{\mathbf{u}^*} \equiv \int \mathrm{d}\mathbf{u}^*$ and $\int_{\mathbf{k}} \equiv \int \mathrm{d}\mathbf{k}$. In the above equation, $\mathbf{u}_b$ and $\mathbf{u}_b^*$ are the velocities of a pair of particles before collision so that the post collisional velocities are $\mathbf{u}$ and $\mathbf{u}^*$, $\mathbf{k}$ is the unit vector in the direction of the line joining the centers of particles at collision, $\mathbf{w} = \mathbf{u} - \mathbf{u}^*$ is the velocity difference between the particles, and the above integral is carried out for $\mathbf{w}\cdot\mathbf{k} \geqslant 0$ so that the particles approach each other prior to collisions. The factor e^{-2} in the first term of the above equation accounts for the

contraction of phase space in a collision due to the inelastic nature of the collision between particles.

The distribution function is determined using an expansion of the form

$$F(\mathbf{u}) = F_0(\mathbf{u}) \left[1 + \sum_{k=1}^{K} A_k \phi_k(\mathbf{u}) \right] , \tag{3}$$

where $F_0(\mathbf{u})$ is the Maxwell–Boltzmann distribution

$$F_0(\mathbf{u}) = \frac{1}{2\pi} \exp\left(-\frac{u^2}{2} \right) . \tag{4}$$

The basis functions ϕ_k are chosen as follows. If an index N is chosen such that polynomials of order $u_x^n u_y^{N-n}$ (for $n \leqslant N$) and of lower order are retained in the expansion, the total number of terms in the expansion is K. Only even values of N are used in the expansion for the base state, to ensure that the resultant basis functions satisfy the underlying symmetry of the distribution function $f(-u_x, -u_y) = f(u_x, u_y)$ for the present case. Of these, it is necessary to consider the equations for mass, momentum and energy separately for reasons explained a little later. The basis functions ϕ_{K-5} to ϕ_K are defined as

$$\begin{aligned}
\phi_{K-5} &= \frac{1}{\sqrt{2}}(u_x^2 - u_y^2) , \\
\phi_{K-4} &= u_x u_y , \\
\phi_{K-3} &= \frac{1}{\sqrt{2}}(u_x^2 + u_y^2) , \\
\phi_{K-2} &= u_x , \\
\phi_{K-1} &= u_y , \\
\phi_K &= 1 .
\end{aligned} \tag{5}$$

The other basis functions, ϕ_1 to ϕ_{K-6}, are defined as

$$\phi_k = He_m(u_x) He_{n-m}(u_y) \tag{6}$$

for $n = 4, 6, \ldots, N$ and $m = 0$ to n, where $k = (\sum_{l=2}^{(n-2)/2} (2l+1)) + m + 1$, and the Hermite polynomials $He_i(x)$ of order i are normalised so that

$$\begin{aligned}
\int_{-\infty}^{\infty} \mathrm{d}x \sqrt{\frac{1}{2\pi}} \exp\left(-\frac{x^2}{2} \right) He_i(x) He_j(x) &= 1 \text{ for } i = j \\
&= 0 \text{ for } i \neq j .
\end{aligned} \tag{7}$$

In expansion 3, the coefficients A_{K-3} to A_K can be set equal to zero without loss of generality, since the basis functions corresponding to these coefficients are the mass, momenta and energy.

The expansion is inserted into the Boltzmann equation, multiplied by $F_0(\mathbf{u})\phi_j(\mathbf{u})$ and integrated over the velocity coordinates to obtain a non-linear vector equation of the form

$$-\gamma(H_i + G_{ij}A_j) = M_i + L_{ij}A_j + N_{ijk}A_jA_k\,, \tag{8}$$

where the summation is carried out over the repeated indices, the $K \times 1$ matrices H_i and M_i are

$$H_i = \int_{\mathbf{u}} \phi_i(\mathbf{u}) \frac{\partial(u_y F_0(\mathbf{u}))}{\partial u_x}\,, \tag{9}$$

$$M_i = \int_{\mathbf{u}} \int_{\mathbf{u}^*} \int_{\mathbf{k}} F_0(\mathbf{u})F_0(\mathbf{u}^*)(\phi_i(\mathbf{u}') - \phi_i(\mathbf{u}))\mathbf{w}\cdot\mathbf{k}\,, \tag{10}$$

the $K \times K$ matrices G_{ij} and L_{ij} are

$$G_{ij} = \int_{\mathbf{u}} \phi_i(\mathbf{u}) \frac{\partial(F_0(\mathbf{u})u_y\phi_j(\mathbf{u}))}{\partial u_x}\,, \tag{11}$$

$$L_{ij} = \int_{\mathbf{u}} \int_{\mathbf{u}^*} \int_{\mathbf{k}} F_0(\mathbf{u})F_0(\mathbf{u}^*)(\phi_j(\mathbf{u}) + \phi_j(\mathbf{u}^*))(\phi_i(\mathbf{u}') - \phi_i(\mathbf{u}))\mathbf{w}\cdot\mathbf{k} \tag{12}$$

and the third order tensor N_{ijk} is

$$N_{ijk} = \int_{\mathbf{u}} \int_{\mathbf{u}^*} \int_{\mathbf{k}} F_0(\mathbf{u})F_0(\mathbf{u}^*)\phi_j(\mathbf{u})\phi_k(\mathbf{u}^*)(\phi_i(\mathbf{u}') - \phi_i(\mathbf{u}))\,, \tag{13}$$

where $\mathbf{u}'$ is the velocity after an inelastic collision of a particle which has a precollisional velocity $\mathbf{u}$ and collides with a particle with velocity $\mathbf{u}^*$ with the unit vector along the line of centers given by $\mathbf{k}$. It can easily be verified that all the terms $L_{(K-2)j} = L_{(K-1)j} = L_{Kj} = N_{(K-2)jk} = N_{(K-1)jk} = N_{Kjk} = 0$ for all j,k due to the mass and momentum conservation in a collision. In addition, $\sum_{j=1}^{K} G_{(K-2)j}A_j = \sum_{j=1}^{K} G_{(K-1)j}A_j = \sum_{j=1}^{K} G_{Kj}A_j = 0$ if $A_{K-3} = A_{K-2} = A_{K-1} = A_K = 0$. Therefore, Eq. (8) for $i = K-2$ to K are identically satisfied. However, Eq. (8) for $i = K-3$ is not identically satisfied, because energy is not a collisional invariant. The $(K-3)$ equations are solved simultaneously to obtain the coefficients A_1 to A_{K-4} and the shear rate γ.

The solution of the simultaneous equations are obtained by defining an auxiliary vector A' of dimension $K-3$ where $A'_i = A_i$ for $k = 1$ to $K-4$, and $A'_{K-3} = \gamma$. The iterative procedure proceeds with an initial guess for this vector, $A_i'^{(0)}$, and the new vector $A_i'^{(n+1)}$ is related to the old vector $A_i'^{(n)}$ by

$$A_i'^{(n+1)} = A_i'^{(n)} - S_{ij}^{(n)}R_j^{(n)}\,, \tag{14}$$

where the $(K-3)$-dimensional vector $R_i^{(n)}$ is the 'remainder' in Eq. (14)

$$R_i^{(n)} = \gamma^{(n)}G_{ij}A_j^{(n)} + L_{ij}A_j^{(n)} + N_{ijk}A_j^{(n)}A_k^{(n)} \tag{15}$$

and $S_{ij}^{(n)}$ is the inverse of the Jacobian at $A_i' = A_i'^{(n)}$

$$(S^{(n)})_{ij}^{-1} = \frac{\partial R_j^{(n)}}{\partial A_i^{(n)}}$$

$$= \gamma^{(n)} G_{ij} + L_{ij} + (N_{ijk} + N_{ikj}) A_k^{(n)} \tag{16}$$

for $i = 1$ to $(K-3)$ and $j = 1$ to $K-4$,

$$(S^{(n)})_{(K-3)j}^{-1} = \frac{\partial R_j^{(n)}}{\partial \gamma^{(n)}}$$

$$= G_{ij} A_j \, . \tag{17}$$

An asymptotic solution for the distribution function in the small parameter $\varepsilon = (1-e)^{1/2}$ can be obtained in the limit $(1-e) \ll 1$. The leading order shear rate is $O(\varepsilon)$ when scaled by $(n\,\mathrm{d}T)$, and the shear rate can be expanded in an asymptotic series

$$\gamma = \varepsilon \gamma^{(1)} + \varepsilon^2 \gamma^{(2)} + \cdots \, . \tag{18}$$

Similarly, the coefficients A_i are expressed as a series in the parameter ε

$$A_i = \varepsilon A_i^{(1)} + \varepsilon^2 A_i^{(2)} + \cdots \, , \tag{19}$$

matrices M_i, L_{ij} and N_{ijk} are also expanded in a series in the parameter ε

$$M_i = M_i^{(0)} + \varepsilon^2 M_i^{(2)} + \varepsilon^4 M_i^{(4)} + \cdots \, ,$$

$$L_{ij} = L_{ij}^{(0)} + \varepsilon^2 L_{ij}^{(2)} + \varepsilon^4 L_{ij}^{(4)} + \cdots \, ,$$

$$N_{ijk} = N_{ijk}^{(0)} + \varepsilon^2 N_{ijk}^{(2)} + \varepsilon^4 N_{ijk}^{(4)} + \cdots \, . \tag{20}$$

In these series, only the terms corresponding to even powers of ε are non-zero because only powers of $(1-e)$ appear in these integrals. In addition, the leading-order elements of these matrices $M_{K-3}^{(0)}$, $L_{(K-3)j}^{(0)}$ and $N_{(K-3)jk}^{(0)}$ corresponding to the energy equation are zero. These series are inserted into Eq. (8) to obtain solutions for the shear rate and the coefficients $A_i^{(n)}$. The leading-order equation is identically satisfied, since the Maxwell–Boltzmann distribution is a solution of the elastic collision operator. The $O(\varepsilon)$ equation is

$$-\gamma^{(1)} H_i = L_{ij}^{(0)} A_j^{(1)} \, . \tag{21}$$

This provides the coefficients $A_i^{(1)}$ in terms of the leading order strain rate $\gamma^{(1)}$ for $i = (1, K-4)$. The equations for $i = (K-3, K)$ are identically satisfied at this order. Note that the strain rate $\gamma^{(1)}$ is as yet unspecified. This is provided by the $O(\varepsilon^2)$ correction to the energy equation (for $i = K-3$). It can easily be verified that $H_{K-3} = 0$, and $N_{(K-3)jk}^{(0)} = L_{(K-3)j}^{(0)} = 0$ for all j,k. Consequently, the leading order energy equation simplifies to

$$\gamma_1 G_{(K-3)j} A_j^{(1)} + M_{K-3}^{(2)} = 0 \, . \tag{22}$$

Table 1

	$K=11$	$K=18$
γ	$3.5012\varepsilon + 2.0318\varepsilon^3 - 0.9789\varepsilon^4$	$3.4967\varepsilon + 2.0590\varepsilon^3 - 0.8654\varepsilon^4$
$\langle u_x u_y \rangle$	$-1.0074\varepsilon + 0.8945\varepsilon^3 - 0.2817\varepsilon^4$	$-1.0078\varepsilon + 0.6411\varepsilon^3 - 0.2494\varepsilon^4$
$\langle u_x^2 - u_y^2$	$2.0671\varepsilon^2 - 1.7088\varepsilon^4$	$2.0756\varepsilon^2 - 0.7058\varepsilon^4$
$\langle u_x^4 \rangle$	$5.2380\varepsilon^2 + 15.3428\varepsilon^4$	$5.1705\varepsilon^2 + 12.9422\varepsilon^4$
$\langle u_x^3 u_y \rangle$	$-2.7853\varepsilon - 3.2221\varepsilon^3 - 2.9190\varepsilon^4$	$-2.7725\varepsilon - 4.3504\varepsilon^3 - 3.4684\varepsilon^4$
$\langle u_x^2 u_y^2 \rangle$	$2.2228\varepsilon^2 - 0.7336\varepsilon^4$	$2.3318\varepsilon^2 - 3.6218\varepsilon^4$
$\langle u_x u_y^2 \rangle$	$-2.7853\varepsilon + 3.9587\varepsilon^3 - 2.7210\varepsilon^4$	$-2.7725\varepsilon + 3.5367\varepsilon^3 - 3.2110\varepsilon^4$
$\langle u_y^4 \rangle$	$-5.3102\varepsilon^2 + 8.9958\varepsilon^4$	$-5.2394\varepsilon^2 - 0.0484\varepsilon^4$

A similar procedure is used for determining the higher corrections to the distribution function.

The corrections to the distribution function have been obtained correct to $O(\varepsilon^4)$ or $(1-e)^2$ in the asymptotic expansion. Two sets of basis functions, one for $K=11$ corresponding to all moments upto fourth order (of the form $u_x^n u_y^{4-n}$ for $0 \leqslant n \leqslant 4$) and one for $K=18$ corresponding to all moments upto sixth order (of the form $u_x^n u_y^{6-n}$ for $0 \leqslant n \leqslant 6$) have been used. The results of the calculation are shown in Table 1. It is seen that the results for the shear rate and the moments of the velocity are in good agreement upto for $K=11$ and $K=18$ upto $O(\varepsilon^3)$, though there is some variation for the $O(\varepsilon^4)$ contributions. This indicates that truncation at fourth moments is not sufficient to capture the $O(\varepsilon^4)$ contribution to the distribution function, and a larger set of moments may be necessary. The results of the present procedure correct to $O(\varepsilon^2)$ were compared with the results of previous studies [3,4] in a previous paper [12]. The results for $K=18$ are used in the stability analysis in the next section.

3. Dispersion relations

In the linear stability analysis, perturbations are imposed on the distribution function of the form

$$f(\mathbf{x},\mathbf{u},t) = F(\mathbf{u}) + f'(\mathbf{x},\mathbf{u},t)\,, \tag{23}$$

where the perturbation $f'(\mathbf{x},\mathbf{u},t)$ has the form

$$f'(\mathbf{x},\mathbf{u},t) = \tilde{f}(\mathbf{u})\exp(\imath k x + \imath l y + s t)\,, \tag{24}$$

where k and l are the wave numbers in the x and y directions, respectively, and s is the growth rate of the perturbations. The above form of the distribution function is inserted into the Boltzmann equation, and linearised about the base state to obtain an equation for the form

$$(s + \imath k u_x + \imath l u_y)\tilde{f} - \gamma \frac{\partial u_y \tilde{f}}{\partial u_x} = \frac{\partial_{cl}\tilde{f}}{\partial t}\,, \tag{25}$$

where the linearised collision integral is given by

$$\frac{\partial_{cl}\tilde{f}}{\partial t} = \int_{\mathbf{u}^*}\int_{\mathbf{k}}\left(\frac{1}{e^2}F(\mathbf{u}_b)\tilde{f}(\mathbf{u}_b^*) + F(\mathbf{u}_b^*)\tilde{f}(\mathbf{u}_b)\right)$$
$$-F(\mathbf{u})\tilde{f}(\mathbf{u}^*) - F(\mathbf{u}^*)\tilde{f}(\mathbf{u}))\mathbf{w}\,.\,\mathbf{k}\,. \tag{26}$$

A series of the following form is assumed for the perturbation to the distribution function $\tilde{f}$:

$$\tilde{f}(\mathbf{u}) = F_0(\mathbf{u})\sum_{i=1}^{K}\tilde{A}_i\phi_i\,, \tag{27}$$

where the basis functions ϕ_i were defined in Eqs. (5) and (6). This series is inserted into Eq. (25), multiplied by the basis function $\phi_i(\mathbf{u})$ and integrated over the particle velocities to get the following matrix equation:

$$(sI_{ij} + \imath kX_{ij} + \imath lY_{ij} - \gamma G_{ij} - C_{ij})\tilde{A}_j = M_{ij}\tilde{A}_j = 0\,, \tag{28}$$

where I_{ij} is the identity matrix, and the other matrices are defined as

$$X_{ij} = \int_{\mathbf{u}} F_0(\mathbf{u})u_x\phi_i(\mathbf{u})\phi_j(\mathbf{u})\,, \tag{29}$$

$$Y_{ij} = \int_{\mathbf{u}} F_0(\mathbf{u})u_y\phi_i(\mathbf{u})\phi_j(\mathbf{u})\,, \tag{30}$$

$$G_{ij} = \int_{\mathbf{u}} F_0(\mathbf{u})\phi_i(\mathbf{u})\left(\frac{\partial u_y\phi_j(\mathbf{u})}{\partial u_x} - u_yu_x\phi_j\right)\,, \tag{31}$$

$$C_{ij} = \sum_{k=1}^{K}A_k\int_{\mathbf{u}}\int_{\mathbf{u}^*}\int_{\mathbf{k}}F_0(\mathbf{u})F_0(\mathbf{u}^*)(\phi_k(\mathbf{u})\phi_j(\mathbf{u}^*) + \phi_k(\mathbf{u}^*)\phi_j(\mathbf{u}))$$
$$\times(\phi_i(\mathbf{u}') - \phi_i(\mathbf{u}))\mathbf{w}\,.\,\mathbf{k}\,. \tag{32}$$

The dispersion relation is obtained by setting the determinant of the matrix M_{ij} equal to zero, so that there are non-trivial solutions for the amplitudes $\tilde{A}_j$.

The calculations are carried out with different values for K, the number of basis functions. For the present study, results have been obtained for $K=15$, $K=21$ and $K=28$, which correspond to retaining all moments upto $(u_x^n u_y^{4-n})$, $(u_x^n u_y^{5-n})$ and $(u_x^n u_y^{6-n})$, respectively. As shown below, it turns out that increasing the number of basis functions has an insignificant effect on the results for the growth rate of the hydrodynamic modes for $e \geqslant 0.9$, though there could be a variation of 5–10% for $0.7 \leqslant e \leqslant 0.9$. However, the scaling behaviour of the hydrodynamic modes is robust, and similar scaling laws are observed for the growth rates even at $e = 0.7$. Calculations have not been done for $e \leqslant 0.7$, because there could be errors in the expressions for the corrections to the distribution function obtained in the previous section.

4. Results

It is first useful to analyse the results for the case of elastic particles, where there is no energy loss during collisions. For a basis set consisting of N functions, there are N solutions for the growth rate. For a system of elastic particles, four of these correspond to the conserved mass, momenta and energy basis functions. In a homogeneous system ($k = 0$), the growth rate corresponding to these four basis functions is equal to zero, while all others are negative. For $k \neq 0$, the growth rates for the transverse momentum and energy modes are diffusive, i.e., they are real and negative and proportional to k^2 for $k \ll 1$, while those for the mass and longitudinal momentum are propagating, i.e., the real part is negative and proportional to k^2 for $k \ll 1$, while the imaginary parts are equal in magnitude and opposite in sign and are proportional to k for $k \ll 1$. These characteristics are captured by the present procedure for obtaining the growth rates, as shown in Fig. 1. Note that the real parts of the growth rates for the hydrodynamic modes are negative, and their magnitudes are shown in Fig. 1. It is also seen that an increase in the number of basis functions from $N = 15$ to 28 results in a small difference in the values of the growth rates in the range $0.01 \leqslant k \leqslant 1.0$. In addition, the expected diffusive behaviour is observed for the density and energy modes and the real part of the velocity modes, while the imaginary parts of the velocity modes increase proportional to k in the limit $k \ll 1$.

The behaviour of the hydrodynamic modes for the granular material in the presence of a shear flow are considered next. The sheared state of the material is anisotropic, and it is necessary to obtain the growth rate separately for the wave numbers k and l. It is first useful to examine the dependence of the results on the number of basis functions K. Fig. 2 shows the results for the growth rate of the diffusive mode, s_d

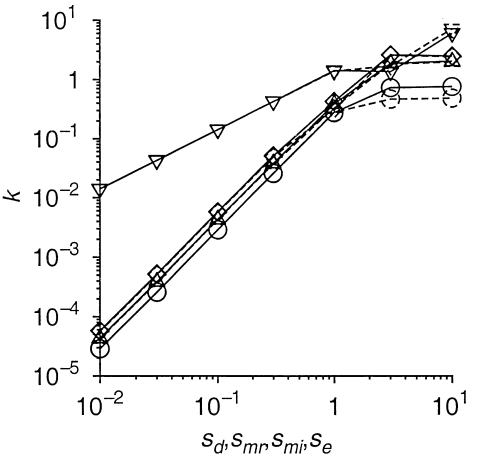

Fig. 1. Variation in the magnitudes of the growth rates of the hydrodynamic modes for a two dimensional gas of elastic particles. (○) s_d; (◇) s_e; (△) s_{mr}; (▽) s_{mi}. The solid lines correspond to the results obtained using 28 basis functions, while the broken lines correspond to result using 15 basis functions.

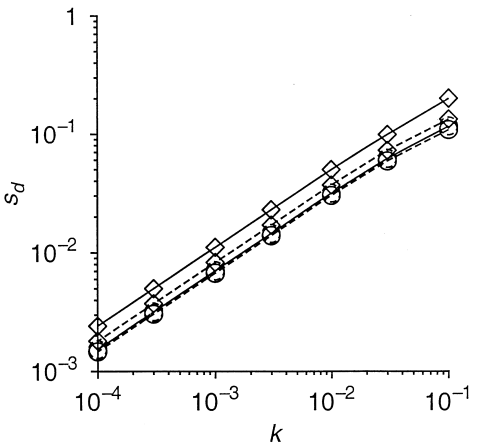

Fig. 2. Variation in the growth rates of the hydrodynamic modes for a two dimensional gas of elastic particles. ($\bigcirc$) $e = 0.9$; ($\diamondsuit$) $e = 0.7$. The solid lines correspond to the results obtained using 28 basis functions, while the broken lines correspond to results using 15 basis functions.

as a function of k for $e = 0.9$ and $e = 0.7$. Similar results are obtained for the other modes as well. It is observed that there is excellent agreement between the results for $K = 15$ and $K = 28$ when the coefficient of restitution is 0.9. The agreement is not as good when the coefficient of restitution is 0.7, but the variation of the growth rate with the wave number shows a similar trend. Thus, though the results of the present analysis show quantitative convergence for $e \geqslant 0.9$, the qualitative trends are preserved as the number of basis functions is increased even for $e = 0.7$. Consequently, the results reported below are obtained using a basis set consisting of 28 functions.

The salient features of the behaviour of the hydrodynamic modes in the flow direction as a function of the wave vector k at $l = 0$ are discussed below.

(1) The growth rate for the transverse momentum mode s_d is real and *positive*, indicating that long wave length perturbations are *unstable* for modes with wave vector along the flow direction. The growth rate is plotted as a function of k in Fig. 3 for different values of the coefficient of restitution e. It can be seen that the scaling of the growth rate of the diffusive mode has the form

$$s_d = s_{dk}|k|^{2/3} \tag{33}$$

for $k \ll 1$, in contrast to the usual hydrodynamic scaling $s_d \propto k^2$ for systems of elastic particles. The variation of the coefficient s_{dk} with the coefficient of restitution is shown in Fig. 7. This coefficient increases as $(1-e)$ increases, and appears to be proportional to $(1-e)^{1/3}$ for $(1-e) \ll 1$. However, there are not enough data points, for reasons mentioned below, in the region $(1-e) \ll 1$ to make a definite assessment.

(2) The real part of the growth rate for the propagating mode s_{mr} turns out to be negative, and $-s_{mr}$ is plotted as a function of k for different values of e in Fig. 4. It is observed here as well that the growth rate has the form

$$s_{mr} = -s_{mrk}|k|^{2/3}\,, \tag{34}$$

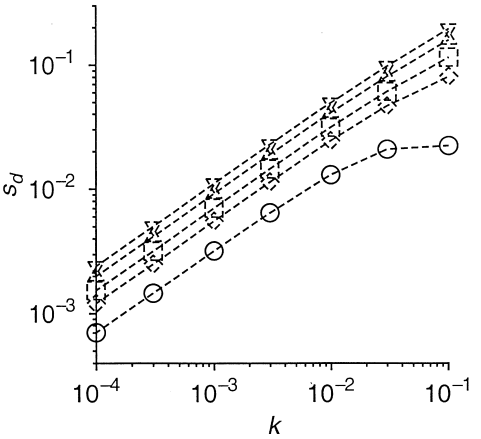

Fig. 3. Variation in s_d as a function of k. ($\bigcirc$) $e = 0.99$; ($\diamond$) $e = 0.95$; ($\square$) $e = 0.9$; ($\triangle$) $e = 0.8$; ($\triangledown$) $e = 0.7$.

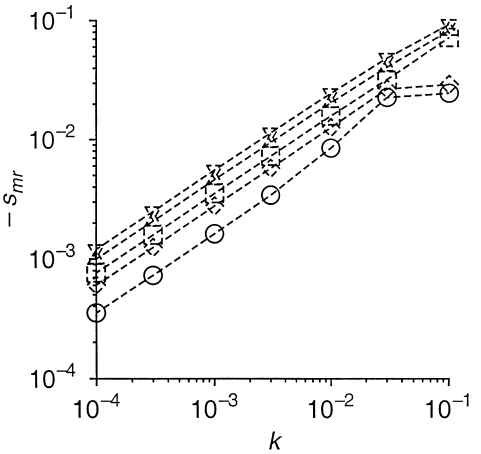

Fig. 4. Variation in $-s_{mr}$ as a function of k. ($\bigcirc$) $e = 0.99$; ($\diamond$) $e = 0.95$; ($\square$) $e = 0.9$; ($\triangle$) $e = 0.8$; ($\triangledown$) $e = 0.7$.

where s_{mrk}, which is a positive coefficient, is shown as a function of e in Fig. 7. This is in contrast to the k^2 scaling for elastic systems. Fig. 7 shows that s_{mrk} increases with increase in $(1-e)$, and scales in a manner similar to s_{dk}.

(3) The imaginary part of the growth rate for the propagating mode, s_{mi}, shown in Fig. 5, is also of the form

$$s_{mi} = \pm s_{mik} |k|^{2/3} , \tag{35}$$

in contrast to the hydrodynamic scaling $s_{mi} \propto k$ in elastic systems. The coefficient s_{mik}, shown as a function of e in Fig. 7, also has a scaling similar to s_{dk} and s_{mrk}.

(4) The growth rate for the energy modes S_e is negative, and converges to a finite value in the limit $k \to 0$ because energy is dissipated in particle collisions. Fig. 6

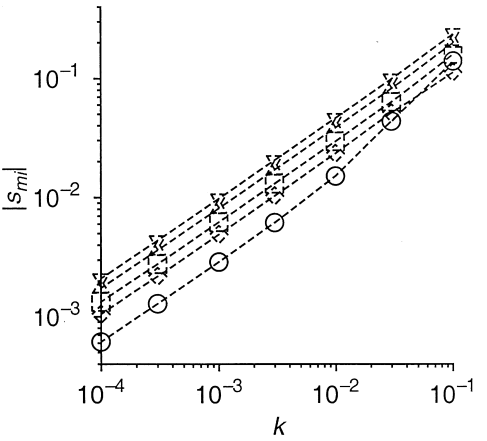

Fig. 5. Variation in $|s_{mi}|$ as a function of k. (○) $e=0.99$; (◇) $e=0.95$; (□) $e=0.9$; (△) $e=0.8$; (▽) $e=0.7$.

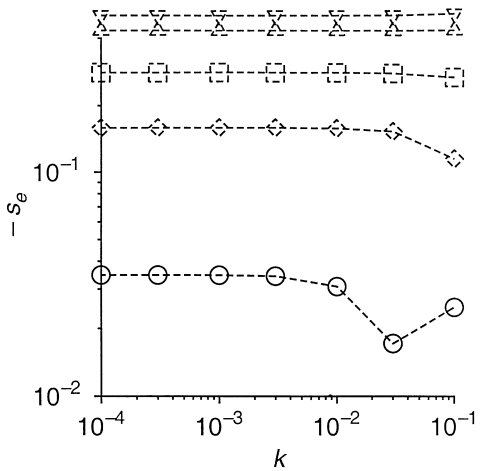

Fig. 6. Variation in $-s_e$ as a function of k. (○) $e=0.99$; (◇) $e=0.95$; (□) $e=0.9$; (△) $e=0.8$; (▽) $e=0.7$.

shows the variation of $-s_d$ as a function of k, and Fig. 7 shows $-s_d$ as a function of e in the limit $k \to 0$.

The variations of the growth rates of the hydrodynamic modes as a function of the wave number l in the direction of shear at $k=0$ is shown in Figs. 8–11. These figures indicate that though there is a quantitative variation in the values of the growth rate, the scaling with l remains unchanged in the limit $l \ll 1$ for the diffusion and momentum modes. The energy mode is, of course, damped.

(1) The growth rate for the transverse momentum mode s_d has the form

$$s_d = -s_{dl} l^2 , \tag{36}$$

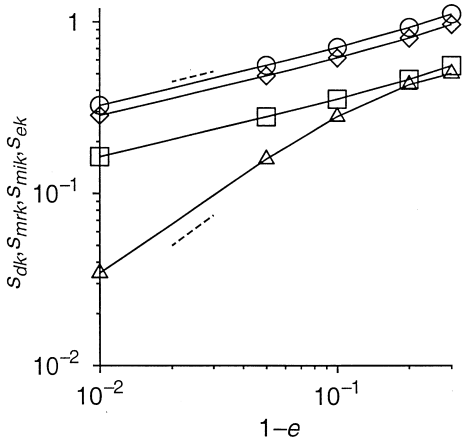

Fig. 7. The coefficients $s_{dk}(\bigcirc)$, $s_{mrk}(\square)$, $s_{mik}(\diamondsuit)$ and $s_{ek}(\triangle)$ as a function of $(1-e)$.

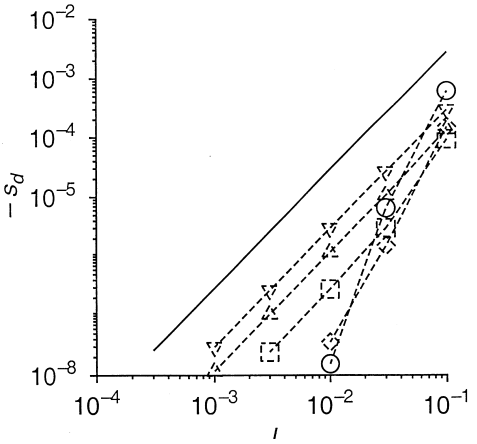

Fig. 8. Variation in $-s_d$ as a function of l. $(\bigcirc)$ $e=0.99$; $(\diamondsuit)$ $e=0.95$; $(\square)$ $e=0.9$; $(\triangle)$ $e=0.8$; $(\bigtriangledown)$ $e=0.7$; (Solid line) $e=1.0$.

as shown in Fig. 8, in the limit $l \ll 1$. This is similar to that for an elastic system. A decrease in the coefficient of restitution tends to decrease the magnitude of the coefficient s_{dl}, which is shown as a function of l in Fig. 12. Moreover, it is apparent from Fig. 12 that the coefficient s_{dl} is small compared to that for an elastic system in the limit $l \ll 1$, the limited data shown in Fig. 12 suggest that the $s_{dl} \sim (1-e)^2$ in the limit $(1-e) \ll 1$. However, there are not enough data points in this limit to make a definite assessment.

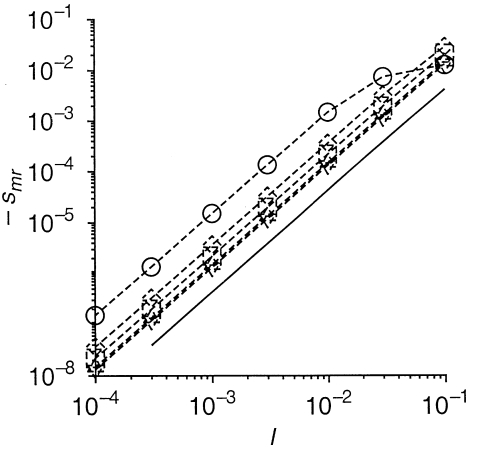

Fig. 9. Variation in $-s_{mr}$ as a function of l. ($\bigcirc$) e=0.99; ($\diamondsuit$) e=0.95; ($\square$) e=0.9; ($\triangle$) e=0.8; ($\triangledown$) e=0.7; (Solid line) $e = 1.0$.

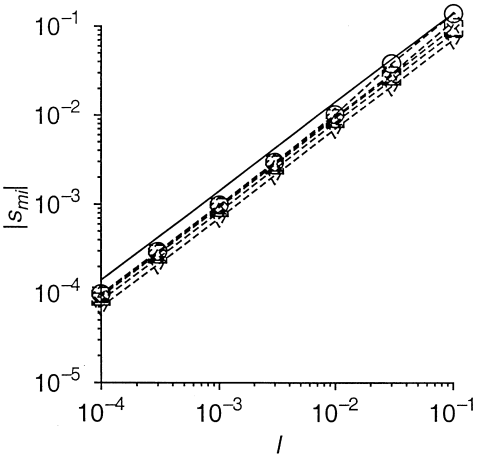

Fig. 10. Variation in $|s_{mi}|$ as a function of l. ($\bigcirc$) $e = 0.99$; ($\diamondsuit$) $e = 0.95$; ($\square$) $e = 0.9$; ($\triangle$) $e = 0.8$; ($\triangledown$) $e = 0.7$; (Solid line) $e = 1.0$.

(2) The real and imaginary parts of the growth rate for the propagating modes, s_{mr} and s_{mi}, are of the form

$$s_{mr} = -s_{mrl} l^2 , \tag{37}$$

$$s_{mi} = \pm s_{mil} l , \tag{38}$$

as shown in Figs. 9 and 10. A decrease in the coefficient of restitution increases the coefficient s_{mrl}, thereby increasing the damping, and Fig. 12 indicates that s_{mrl} increases proportional to $(1-e)^{-1}$ while s_{mil} tends to a constant value in the limit $(1-e) \ll 1$.

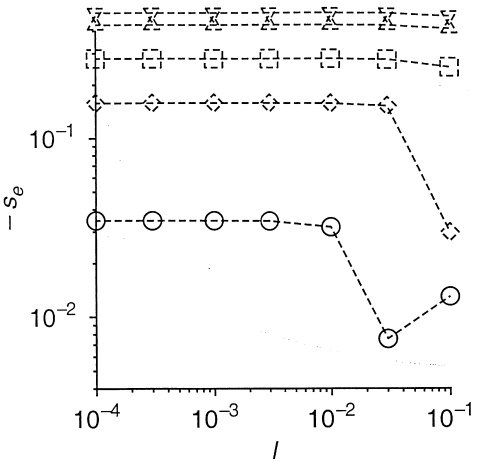

Fig. 11. Variation in $-s_e$ as a function of l. ($\bigcirc$) e=0.99; ($\diamondsuit$) e=0.95; ($\square$) e=0.9; ($\triangle$) e=0.8; ($\triangledown$) e=0.7; (Solid line) $e = 1.0$. The dashed lines, from bottom to top, show slopes of ($\frac{1}{3}$) and 1, respectively.

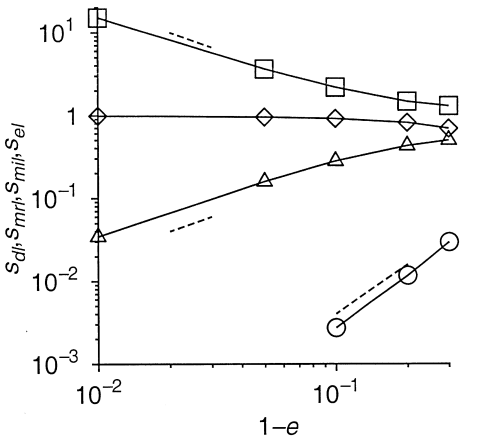

Fig. 12. The coefficients s_{dl} ($\bigcirc$), s_{mrl} ($\square$), s_{mil} ($\diamondsuit$) and s_{el} ($\triangle$) as a function of $(1-e)$. The dashed lines, from bottom to top, show slopes of 2, 1 and -1, respectively.

(3) The growth rate of the mode corresponding to total energy, s_e, is damped because energy is not conserved in collisions, as shown in Fig. 11. The variation of the growth rate in the limit $l \ll 1$, shown in Fig. 12, is similar to the variation of s_e in the limit $k \ll 1$.

It should be noted that the scaling relations obtained from Figs. 7 and 12 are approximate, since it was not possible to extend the numerical results to $(1-e) < 0.01$ for reasons mentioned below.

The above results show a qualitative variations in the growth rates when the coefficient of restitution is changed from 1.0 to 0.99. In this case, it is of interest to

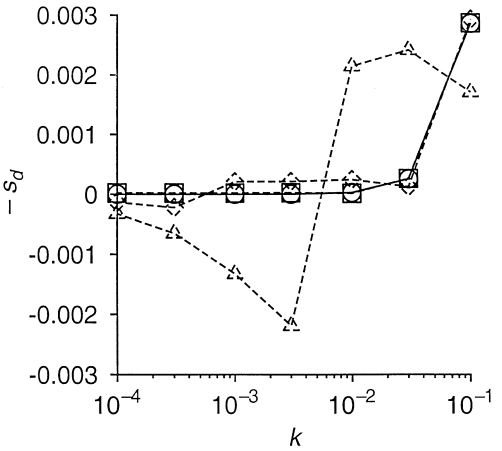

Fig. 13. The growth rate $-s_d$ as a function of k for (○) $(1-e)=10^{-6}$; (□) $(1-e)=10^{-5}$; (◇) $(1-e)=10^{-4}$; (△) $(1-e)=10^{-3}$.

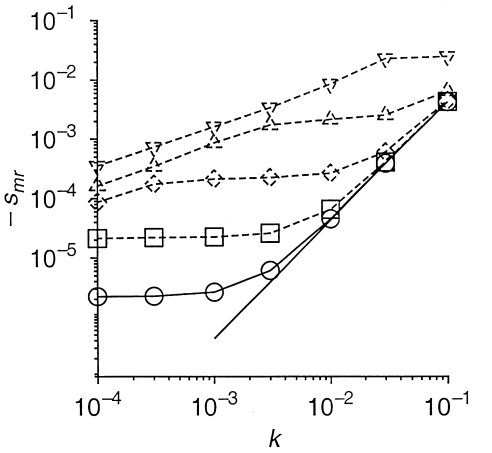

Fig. 14. The growth rate $-s_{mr}$ as a function of k for (○) $(1-e)=10^{-6}$; (□) $(1-e)=10^{-5}$; (◇) $(1-e)=10^{-4}$; (△) $(1-e)=10^{-3}$; (▽) $(1-e)=10^{-2}$; (Solid line) $e=1$.

determine whether the change in scaling laws is discontinuous, or whether there is a continuous variation in the scaling behaviour as e is decreased from 1. Figs. 13–15 show the variation in s_d, s_{mr} and s_{mi} for $(1-e)=10^{-6}$, 10^{-5}, 10^{-4} and 10^{-3}. It is observed that at $(1-e)=10^{-6}$, the coefficients are indistinguishable from those at $e=1$, while in the other cases the coefficients are close to those at $e=1$ for larger values of k while they show significant deviation at small values of k. This indicates that the scaling does show a continuous variation from those for a conservative system to those obtained above for an inelastic system in a continuous fashion. However, for

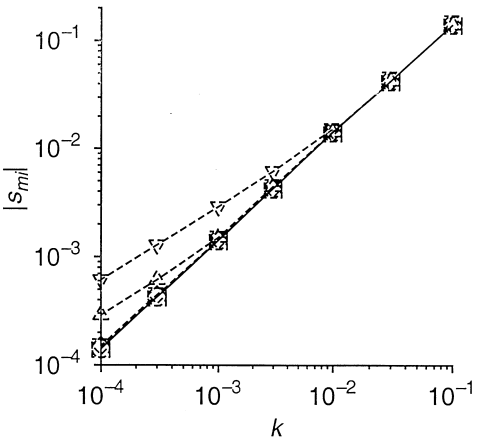

Fig. 15. The growth rate $|s_{mi}|$ as a function of k for ($\bigcirc$) $(1-e)=10^{-6}$; ($\square$) $(1-e)=10^{-5}$; ($\diamondsuit$) $(1-e)=10^{-4}$; ($\triangle$) $(1-e)=10^{-3}$; ($\triangledown$) $(1-e)=10^{-2}$; (Solid line) $e=1$.

values of the coefficient of restitution that are encountered in practical systems, the scaling is very different from that for elastic systems.

5. Conclusions

The growth rates for the hydrodynamic modes of the two-dimensional homogeneous shear flow of inelastic disks were determined by solving the Boltzmann equation. The diameter of a disk was considered to be small compared to the mean-free path, and the only length scale is the mean-free path $(1/n\,\mathrm{d}T^{1/2})$, where n is the number of disks per unit area and T is the mean square velocity of the disks. In addition, there is only one time scale, the strain rate of the mean flow γ, which can be related to the mean square velocity of the disks T. All lengths are non-dimensionalised by the mean-free path and velocities by $\sqrt{T}$ in the Boltzmann equation, and the only variable parameter in the resultant equation is the coefficient of restitution e. The velocity distribution in the homogeneous sheared state of the system is determined using an expansion in a set of basis functions. In addition, an expansion in the parameter $\varepsilon=(1-e)^{1/2}$ is used to simplify the calculation, and terms correct to $\mathrm{O}(\varepsilon^4)$ are retained in the expansion. The results indicate that this solution could result in errors of about 5% at $e=0.7$ due to the neglect of higher-order terms.

The dispersion relation for the growth rate of the hydrodynamic modes was determined by placing a small perturbation on the steady solution of the Boltzmann equation. An expansion in a set of basis functions was used, and it was found that the results for the hydrodynamic modes are independent of the number of basis functions K for $K=15, 21$ and 28. The subsequent calculations were carried out using 28 basis functions. The results indicate that the scaling laws for the hydrodynamic modes are very

different from those for systems of elastic particles. In the flow direction, the transverse momentum mode is unstable, and the growth rate increases as $s_d \propto k^{2/3}$ in the limit $k \to 0$. The propagating mode is stable, but its real and imaginary parts also increase as $k^{2/3}$. The mode corresponding to energy fluctuations is stable, and the decay rate converges to a finite value in the limit $k \to 0$. In the direction of shear, the hydrodynamic modes have a behaviour similar to those in a system of elastic disks, but the decay rate of the diffusive mode is much lower than that in an elastic system, while that for the propagating mode is higher.

While equations similar to the Navier–Stokes equation (for simple fluids) have been extensively used to model the sheared state of a granular material, relatively little work has been done on the derivation of the macroscopic equations from a microscopic description. The Navier–Stokes type models contain approximations for the constitutive relations which are based on kinetic theories for systems of elastic particles, and the implicit assumption in these models is that the dispersion relation for the hydrodynamic modes about the sheared steady state is similar to that for a gas of elastic particles at equilibrium. In the present analysis, the Boltzmann equation was solved to obtain the steady-state solution for the velocity distribution, and the dispersion relation for this steady distribution was determined. Though the Boltzmann equation already contains assumptions such as the molecular chaos assumption (the pair distribution function is the product of single particle distributions), the results indicate that the behaviour of the sheared steady state of a system of inelastic disks is qualitatively different from that for an elastic system. Though the behaviour of the sheared state does converge to that of a system of elastic disks, this is restricted to coefficients of restitution in the range $0.999999-0.9999$, and the anomalous behaviour of the hydrodynamic modes is clearly seen for $e \leqslant 0.99$. This seems to suggest that the form of the macroscopic transport equations for the hydrodynamic variables in the sheared state for realistic values of the coefficient of restitution could be very different from that for simple fluids. However, the present results are restricted to a dilute system of disks in two dimensions, and it is necessary to do further analysis for three-dimensional systems at higher densities.

The reason for the anomalous behaviour of the hydrodynamic modes is likely to be different from that observed in other systems. In the area of dynamical critical phenomena, for example, anomalous behaviour of transport coefficient is observed only very near critical points, due to the divergence of thermodynamic susceptibility near the critical point [13]. Collective effects could also result in anomalous behaviour, such as the long time tail in viscous systems [14]. The characterisitc frequency in turbulent flows [15] in the inertial sub range varies proportional to $k^{2/3}$ due to the presence of multiple scales across which the energy flux remains unchanged. However, since there is no underlying equilibrium state in the present case, the Boltzman equation considers only pair interactions between particles. The only possible reason for this anomalous behaviour seems to be the inelasticity of interparticle collisions, and the connection between the inelasticity of particle collisions and the anomalous behaviour of hydrodynamic modes remains to be elucidated.

References

[1] J.T. Jenkins, S.B. Savage, A theory for rapid flow of identical, smooth, nearly elastic, spherical particles, J. Fluid Mech. 130 (1983) 187.
[2] C.K.K. Lun, S.B. Savage, D.J. Jeffrey, N. Chepurniy, Kinetic theories of granular flow: inelastic particles in a Couette flow and slightly inelastic particles in a general flow field, J. Fluid Mech. 140 (1984) 223.
[3] J.T. Jenkins, M.W. Richman, Grad's 13 moment system for a dense gas of inelastic particles, Arch. Rat. Mech. Anal. 87 (1985) 355.
[4] N. Sela, I. Goldhirsch, S.H. Noskowicz, Kinetic theoretical study of a simply sheared two dimensional granular gas to Burnett order, Phys. Fluids 8 (1996) 2337.
[5] J.T. Jenkins, M.W. Richman, Boundary conditions for plane flows of smooth, nearly elastic, circular disks, J. Fluid Mech. 171 (1986) 53.
[6] M.A. Hopkins, M.Y. Louge, Inelastic microstructure in rapid granular flows of smooth disks, Phys. Fluids A 3 (1991) 47.
[7] S.B. Savage, Instability of unbounded uniform granular shear flow, J. Fluid Mech. 241 (1992) 109.
[8] M. Babic, On the stability of rapid granular flows, J. Fluid Mech. 254 (1993) 127.
[9] P.J. Schmid, H.K. Kytomaa, Transient and asymptotic stability of a granular shear flow, J. Fluid Mech. 264 (1994) 255.
[10] C.-H. Wang, R. Jackson, S. Sundaresan, Stability of bounded rapid shear flows of a granular material, J. Fluid Mech. 308 (1996) 31.
[11] P. Resibois, M. de Leener, Classical Kinetic Theory of Fluids, Wiley, New York, 1977.
[12] V. Kumaran, Asymptotic solution of the Boltzmann equation for the shear flow of smooth inelastic disks, Physica A 275 (2000) 483.
[13] P.C. Hohenberg, B.I. Halperin, Rev. Mod. Phys. 49 (1977) 435.
[14] J.-P. Hansen, I. McDonald, Theory of Simple Liquids, Academic Press, London, 1996.
[15] H. Tennekes, J.L. Lumley, A First Course in Turbulence, MIT Press, Cambridge, 1972.